ANTIMICROBIAL AGENTS AND CHEMOTHERAPY, May 2006, p. 1841–1851 Vol. 50, No. 5
0066-4804/06/$08.00+0 doi:10.1128/AAC.50.5.1841–1851.2006

Functional Characterization and Target Validation of Alternative Complex I of *Plasmodium falciparum* Mitochondria

Giancarlo A. Biagini,[1]* Parnpen Viriyavejakul,[1] Paul M. O'Neill,[2] Patrick G. Bray,[1] and Stephen A. Ward[1]*

Liverpool School of Tropical Medicine, Pembroke Place, Liverpool L35 QA,[1] and Departments of Chemistry and Pharmacology, University of Liverpool, Liverpool L69 7ZD,[2] United Kingdom

Received 24 January 2006/Accepted 3 February 2006

This study reports on the first characterization of the alternative NADH:dehydrogenase (also known as alternative complex I or type II NADH:dehydrogenase) of the human malaria parasite *Plasmodium falciparum*, known as PfNDH2. PfNDH2 was shown to actively oxidize NADH in the presence of quinone electron acceptors CoQ_1 and decylubiquinone with an apparent K_m for NADH of approximately 17 and 5 μM, respectively. The inhibitory profile of PfNDH2 revealed that the enzyme activity was insensitive to rotenone, consistent with recent genomic data indicating the absence of the canonical NADH:dehydrogenase enzyme. PfNDH2 activity was sensitive to diphenylene iodonium chloride and diphenyl iodonium chloride, known inhibitors of alternative NADH:dehydrogenases. Spatiotemporal confocal imaging of parasite mitochondria revealed that loss of PfNDH2 function provoked a collapse of mitochondrial transmembrane potential (Ψ_m), leading to parasite death. As with other alternative NADH:dehydrogenases, PfNDH2 lacks transmembrane domains in its protein structure, and therefore, it is proposed that this enzyme is not directly involved in mitochondrial transmembrane proton pumping. Rather, the enzyme provides reducing equivalents for downstream proton-pumping enzyme complexes. As inhibition of PfNDH2 leads to a depolarization of mitochondrial Ψ_m, this enzyme is likely to be a critical component of the electron transport chain (ETC). This notion is further supported by proof-of-concept experiments revealing that targeting the ETC's Q-cycle by inhibition of both PfNDH2 and the bc_1 complex is highly synergistic. The potential of targeting PfNDH2 as a chemotherapeutic strategy for drug development is discussed.

New empirical estimates put the number of episodes of clinical *Plasmodium falciparum* malaria in the range of half a billion per year (44). It is estimated that, from these infections, approximately 2.7 million deaths occur per year, mostly among young children under the age of five (6). Unfortunately, these staggering figures are on the increase, largely as a result of parasite multidrug resistance (45). A number of strategies have been proposed to deal with this global health problem, one of which is the development of novel drugs for new parasite targets (4).

In search of new antimalarial drug targets, we have focused on the electron transport chain (ETC) of the malaria parasite mitochondrion. The recently completed malaria genome project revealed that *P. falciparum* mitochondria lack the conventional rotenone-sensitive complex I (or NADH:dehydrogenase) found in most mammalian mitochondria but instead contain an alternative complex I (or type II NADH:dehydrogenase) (22). The activity of this enzyme has yet to be biochemically confirmed in the human malaria parasite *P. falciparum*; however, it has recently been detected in the rodent malaria parasite *Plasmodium yoelii* (49). Alternative NADH:dehydrogenases have been described in some detail for plants, fungi, and bacteria (25, 32, 33, 36, 40, 53). Type II NADH:dehydrogenases are rotenone insensitive and are not proton pumping but nevertheless provide a mechanism for removal of excess reducing power to balance the redox state of the cell (32, 36, 39, 40). Depending on whether the type II NADH:dehydrogenases are localized on the internal or the external face of the inner mitochondrial membrane, they are able to recycle mitochondrial matrix or cytosolic NAD(P)H, respectively. Importantly, a recent bioinformatic study has identified the type II NADH:dehydrogenase of *P. falciparum* as a putative "choke point" in the mitochondrial ETC (54), supporting our hypothesis that this enzyme may indeed provide an attractive chemotherapeutic target.

Targeting the mitochondrial ETC of the human malaria parasite has already been shown to be a successful chemotherapeutic strategy. *P. falciparum* mitochondria use a different homolog of ubiquinone (CoQ_8) than their mammalian host (42, 43), and several antimalarial drugs show specificity for parasite CoQ, including the hydroxynaphthoquinones (13, 50). This strategy led to the development of atovaquone (20), an inhibitor of complex III (or bc_1 complex), which has been successful clinically, especially in combination with proguanil (Malarone), for the treatment of chloroquine-resistant infections (31).

The physiological consequences of targeting the malaria parasite mitochondrial ETC are not well understood. Part of this problem is that the function of malaria parasite mitochondria is regarded as somewhat enigmatic. It is known, for example, that these mitochondria are able to generate a large transmembrane potential (Ψ_m), as demonstrated by the accumulation of cationic fluorescent probes (for examples, see references 12 and 46). However, although recent evidence in rodent malaria parasites suggests that the large mitochondrial Ψ_m is able to

* Corresponding author. Mailing address: Liverpool School of Tropical Medicine, Pembroke Place, Liverpool L35QA, United Kingdom. Phone: 44 1517053151. Fax: 44 1517053371. E-mail for Giancarlo A. Biagini: Biagini@liv.ac.uk. E-mail for Stephen A. Ward: saward@liv.ac.uk.

drive the synthesis of ATP (48, 49), it is still widely accepted that the majority of the parasite's ATP demand is met through glycolysis (21).

It is more likely then that the mitochondrion of the malaria parasite is vital for other cellular functions. Evidence is emerging that, as with mammalian mitochondria, these functions are likely to involve a role in cellular Ca^{2+} homeostasis (23, 48) as well as the de novo synthesis of pyrimidine through the activity of dihydroorotate dehydrogenase (26, 27).

In this study, we report for the first time on (i) the biochemical characterization of the *P. falciparum* type II NADH:dehydrogenase (PfNDH2), (ii) the role of PfNDH2 in mitochondrial function, and (iii) the pharmacological validation of PfNDH2 as a chemotherapeutic target. Implications of these new data on parasite bioenergetics, physiology and chemotherapy are discussed.

MATERIALS AND METHODS

Parasite, culture, and drug sensitivity assays. *P. falciparum* strain TM6 (chloroquine resistant) was obtained from P. Tan-Ariya (Mahidol University, Bangkok, Thailand) and maintained in continuous culture. Cultures contained a 2% suspension of O+ erythrocytes in RPMI 1640 medium (R8758, glutamine, and $NaHCO_3$) supplemented with 10% pooled human AB+ serum, 25 mM HEPES (pH 7.4), and 20 μM gentamicin sulfate (47). Cultures were grown under a gaseous headspace of 4% O_2 and 3% CO_2 in N_2 at 37°C. Parasite growth was synchronized by treatment with sorbitol (29). The sensitivity of *P. falciparum*-infected erythrocytes to various drugs was determined using the [^{3}H]hypoxanthine incorporation method (10) with an inoculum size of 0.5% parasitemia (ring stage) and 1% hematocrit. IC_{50}s (50% inhibitory concentrations) were calculated by using the four-parameter logistic method (Grafit program; Erithacus Software, United Kingdom). To determine whether the antimalarial activity of two drugs is additive, antagonistic, or synergistic, parasite growth was tested by titration of the two drugs at fixed ratios proportional to their IC_{50}s. The fractional inhibitory concentrations of the resulting IC_{50}s were plotted as isobolograms (2).

NADH:quinone oxidoreductase enzyme activity. PfNDH2 activity was determined based on a modification of the NADH:quinone oxidoreductase assay described by Lenaz et al. (30). Free parasites were prepared from aliquots of infected erythrocytes (approximately 8×10^9 cells/ml) by adding 5 volumes of 0.15% (wt/vol) saponin in phosphate-buffered saline (137 mM NaCl, 2.7 mM KCl, 1.76 mM K_2HPO_4, 8.0 mM Na_2HPO_4, 5.5 mM D-glucose, pH 7.4) for 5 min, followed by three washes by centrifugation and resuspension in HEPES (25 mM)-buffered RPMI and a final resuspension in distilled water containing a protease inhibitor cocktail (Complete Mini; Roche). Cell extract was prepared by repeated freeze-thawing in liquid N_2, followed by disruption with a sonicating probe. Enzyme activity was measured in a buffered solution containing KCl (50 mM), Tris-HCl (10 mM, pH 7.4), EDTA (1 mM), KCN (2 mM), and atovaquone (10 μM) with either coenzyme Q_1 (CoQ_1) or decylubiquinone (DB) (200 μM). KCN and atovaquone were added to avoid the electron flow through the cytochrome system (complexes III and IV). A final assay concentration of 600 μM NADH was used for inhibitor studies. The reaction was initiated by the addition of cell extract (approximately 500 μg protein), and activity was monitored spectrophotometrically by monitoring the decrease in absorbance at 340 nm (NADH $\varepsilon = 6.22$ mM). Enzyme kinetic parameters were calculated using Grafit software (Erithacus Software, United Kingdom).

Real-time single-cell monitoring of membrane potential (Ψ_m). The rhodamine derivative TMRE (tetramethyl rhodamine ethyl ester) was used to monitor the membrane potential (Ψ_m) of the plasma membrane and mitochondria of malaria-infected red blood cells. TMRE is cationic and reversibly accumulates inside energized membranes according to the Nernst equation. For experimentation, suspensions (1%) of infected erythrocytes in HEPES-buffered RPMI medium (no serum) were loaded with TMRE (250 nM; Molecular Probes) for 10 min at 37°C. For imaging, malaria parasite-infected erythrocytes were immobilized using polylysine-coated coverslips in a Bioptechs FCS2 perfusion chamber and maintained at 37°C in growth medium (no serum). Inhibitors were added to the perfusate, and the membrane potential-dependent fluorescence responses were monitored in real time. During all manipulations, the concentration of TMRE in the perfusate was kept at 250 nM. The fluorescence signals from malaria-infected erythrocytes were collected on a Zeiss Pascal confocal laser scanning microscope through a Plan-Apochromat 63× 1.2 numerical aperture water objective. Excitation of TMRE was performed using the HeNe laser line at 543 nm. Emitted light was collected through a 560-nm long pass filter from a 543-nm dichroic mirror. Photobleaching (the irreversible damage of TMRE producing a less fluorescent species) was assessed by continuous exposure (5 min) of loaded cells to laser illumination. For each experiment, the laser illumination and microscope settings that gave no reduction in signal were used. Data capture and extraction were carried out with Zeiss Pascal software and Photoshop.

RESULTS

***P. falciparum* displays rotenone-insensitive NADH:quinone reductase activity.** Isolation of ETC enzymes in their active form is a notoriously difficult task (30); therefore, we determined the quinone-dependent oxidation of NADH in situ in cell extracts of freed *P. falciparum* parasites. The reaction was functionally isolated from other respiratory complexes by the action of atovaquone and cyanide for complexes III and IV, respectively. The native ubiquinone of *P. falciparum* is CoQ_8 (42, 43), but as this is too hydrophobic and cannot be used as an exogenous substrate, we assayed PfNDH2 activity using the more hydrophilic short-chain analogs CoQ_1 (with only one isoprenoid unit in the side chain) and DB, which contains a 10-carbon linear saturated side chain. Quinone-dependent oxidation of NADH displayed Michaelis-Menten kinetics (Fig. 1A) with an apparent K_m of 16 and 5 μM for NADH with CoQ_1 and DB, respectively (Table 1). PfNDH2 activity was shown to be insensitive to rotenone (50 μM), the well-known inhibitor of mammalian complex I (9), but sensitive to the flavin reagents diphenylene iodonium chloride (DPI) and diphenyl iodonium chloride (IDP), known type II NADH:dehydrogenase inhibitors (15–18). Inhibition kinetics of PfNDH2 activity with DPI are presented for both electron acceptors CoQ_1 and DB (Table 1 and Fig. 1B). With DB as the electron acceptor, IDP was observed to inhibit PfNDH2 activity with an IC_{50} of 66 ± 18 μM.

Dynamic single-cell measurement of plasma membrane and mitochondrial membrane potential (Ψ_m). To determine the physiological consequence of inhibiting PfNDH2 activity, we set up a real-time single-cell imaging assay for the measurement of mitochondrial membrane potential (Ψ_m). The measurement of mitochondrial Ψ_m is based on the accumulation of the cationic fluorescence probe TMRE (see Materials and Methods) according to the Nernst equation. High fluorescence denotes a high Ψ_m. As with all fluorescence probes, dynamic measurements of fluorescence are prone to photobleaching. A number of parameters on the confocal laser scanning microscope can be easily regulated to minimize photobleaching; these include laser power (both voltage settings and attenuation [%]), scan speed, pinhole diameter, number of scan sweeps, and degree of magnification. At the beginning of every experiment, these parameters were optimized to prevent photobleaching during the course of the experiment; thus, all the figures demonstrating a reduction in fluorescence correspond to a reduction in Ψ_m.

Upon addition of TMRE to *P. falciparum*-infected erythrocytes, a strong fluorescence signal could be observed originating from the parasite cytosol denoting the existence of a high Ψ_m (Fig. 2a and b). This observation was expected, as the plasma membrane of *P. falciparum* is known to have a high Ψ_m

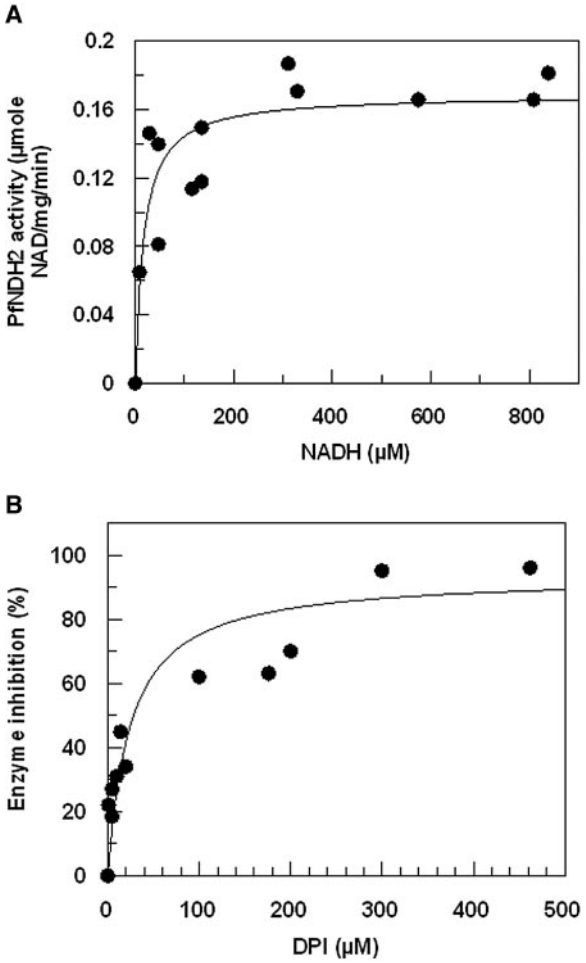

FIG. 1. Kinetics of alternative complex I (PfNDH2) activity in *P. falciparum*. (A) Concentration dependence of rotenone-insensitive oxidation of NADH in cell-free parasite extracts with CoQ_1 as an exogenous substrate. Data points are means of results from three individual experiments. (B) Concentration-dependent DPI inhibition of PfNDH2 enzyme activity with CoQ_1 as an exogenous substrate. Data points are means from duplicate observations from three individual experiments. Data were fitted to a function describing simple ligand binding at a single site by nonlinear regression analysis (Marquart method) using an iterative procedure to generate the best fit (χ^2) of the curve to the data. Standard errors were calculated for each parameter using the matrix inversion method (Grafit user manual).

of approximately −100 mV generated by the action of a proton-pumping V-type ATPase (1). Upon addition of the V-type H^+ ATPase inhibitors bafilomycin A_1 or concanomycin (200 nM), approximately 70 to 80% of the fluorescence signal was lost (Fig. 3A and B), leaving a small but strong signal originating from the parasite mitochondrion (Fig. 2c, d, and e). As observed in earlier studies (12, 51), the morphology of the mitochondria varied considerably according to the stage in the parasite cell cycle, appearing either short and condensed (Fig. 2c), long and stringy (Fig. 2d), or segmented, especially in late trophozoites (Fig. 2e). Merozoites were also shown to yield a strong fluorescence signal and a small rod-like structure, which we have assumed to be the mitochondrion (Fig. 2f).

Additions of known mitochondrial ETC inhibitors such as cyanide (at 1 or 10 mM), azide (10 mM, not shown), and atovaquone (10 μM) were shown to reduce total parasite fluorescence by 20 to 30% (Fig. 3C and D). Fluorescence signals from bafilomycin- or concanomycin-treated parasites, i.e., mitochondrial fluorescence, were completely depleted upon addition of mitochondrial ETC inhibitors (e.g., cyanide [10 mM], azide [10 mM] [not shown], and atovaquone [10 μM]) (Fig. 4C). A complete loss of parasite fluorescence signal was also achieved by the addition of the H^+ ionophore FCCP [carbonyl cyanide *p*-(trifluoromethyl) phenylhydrazone] (Fig. 3A, B, C, and D).

Since both the plasma membrane and the mitochondrion Ψ_m contribute to the accumulation of TMRE, we could not accurately quantify the finite Ψ_m values, as previously reported for amitochondriate cells (3). Therefore, for all experiments, the fluorescence dynamic range was set up so that untreated TMRE-loaded cells were regarded as having complete fluorescence (100%), while the baseline (0%) was set by addition of FCCP. For mitochondrial-dependent fluorescence, bafilomycin A_1-treated cells were normalized to 100% and, again, the baseline (0%) was set by FCCP.

Inhibition of PfNDH2 collapses mitochondrial Ψ_m. The Ψ_m-dependent fluorescence of either untreated or bafilomycin-treated infected erythrocytes was shown to be insensitive to the NADH:dehydrogenase inhibitor rotenone (50 μM) (Fig. 4A and C) or to the alternative oxidase inhibitor SHAM (Fig. 4B) (38). However, addition of flavone did decrease the mitochondrial component of the parasite fluorescence signal (Fig. 4D). The type II NADH:dehydrogenase inhibitor DPI was also shown to reduce the mitochondrial component of the TMRE fluorescence signal, as indicated by the reduction of only the bafilomycin-insensitive component of fluorescence (Fig. 5A and B). The inhibition of mitochondrial Ψ_m by DPI was observed to be both time and dose dependent and saturable with an IC_{50} for the initial rate of inhibition measured at ~3 μM (Fig. 5C). A similar inhibition of mitochondrial Ψ_m was also observed by the related flavin reagent IDP (data not shown). It should be stressed that both DPI and IDP were shown to reduce the mitochondrial membrane potential at a concentration of ≥1 μM. At concentrations below 1 μM, it was not always possible to differentiate between drug-induced reductions of mitochondrial fluorescence and reductions in fluorescence caused by the small but inevitable effect of photobleaching. Similarly, it was not always possible to observe a depolarization of the mitochondrial membrane potential by atovaquone at a concentration below 100 nM. It is likely, therefore, that our measurements underestimate the inhibitory potential of these drugs against mitochondrial function. This is

TABLE 1. Catalytic activity and inhibitory profile of PfNDH2 with different electron acceptors[a]

Acceptor	V_{max} (μmol min^{-1} mg^{-1})	Apparent K_m for NADH (μM)	DPI IC_{50} (μM)
CoQ_1	0.16 ± 0.01	16.7 ± 7.5	24.5 ± 8.6
DB	0.12 ± 0.01	5.1 ± 2.0	15.5 ± 6.6

[a] Values are means ± standard errors of results from independent experiments (n = 3).

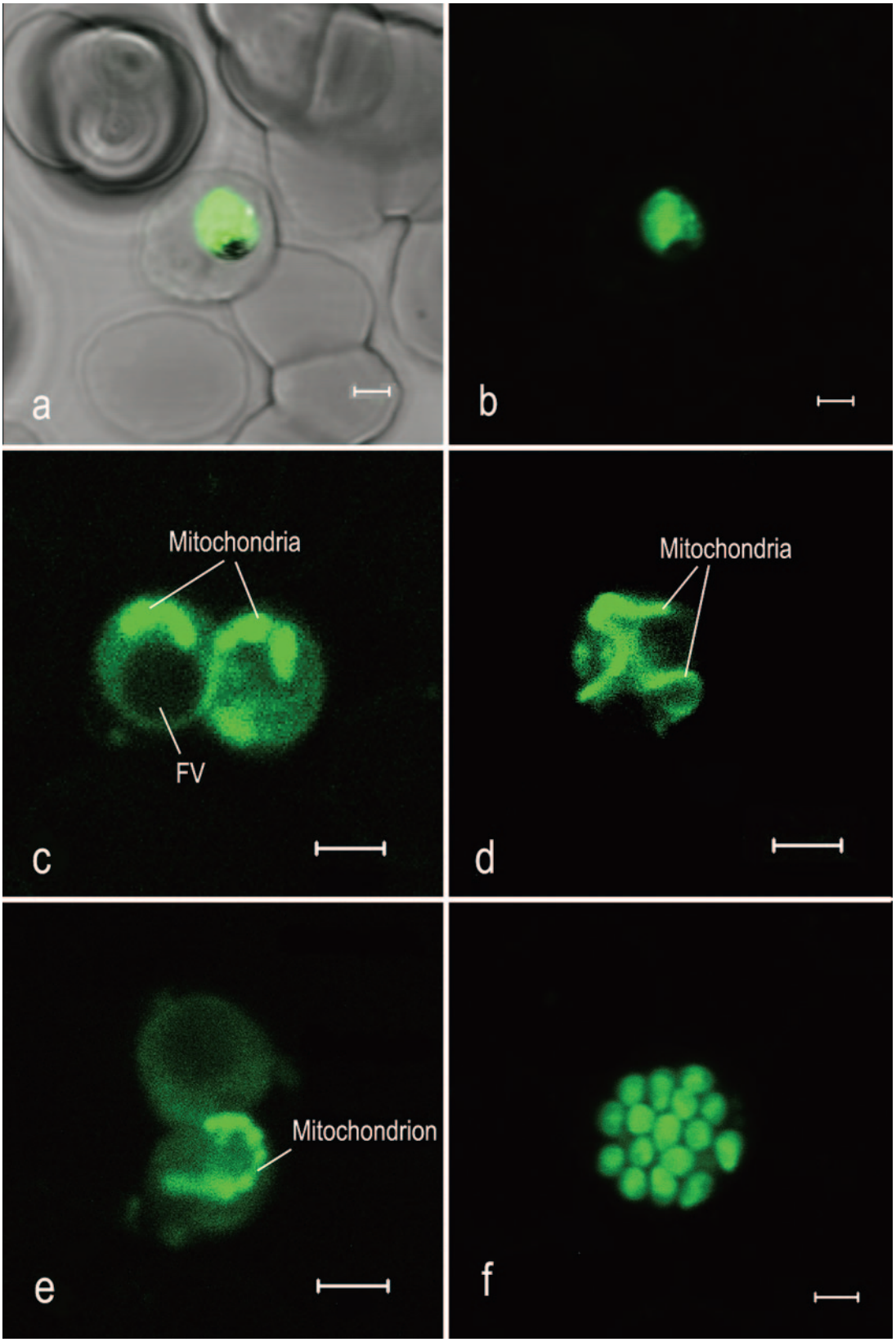

FIG. 2. The plasma and mitochondrial membranes of *P. falciparum* generate a high transmembrane electrochemical potential (Ψ_m). Confocal laser scanning microscopy of live *P. falciparum*-infected erythrocytes loaded with the potentiometric probe TMRE. The panels show bright-field fluorescence (a) and fluorescence (b) images of an infected erythrocyte loaded with TMRE, TMRE fluorescence of parasite mitochondria from bafilomycin-treated parasites (c, d, and e), and TMRE fluorescence from merozoites (f). The green in these images is a pseudocolor. TMRE was excited at 543 nm, and emission was collected with a 560-nm long pass filter. Bars, 2 μm.

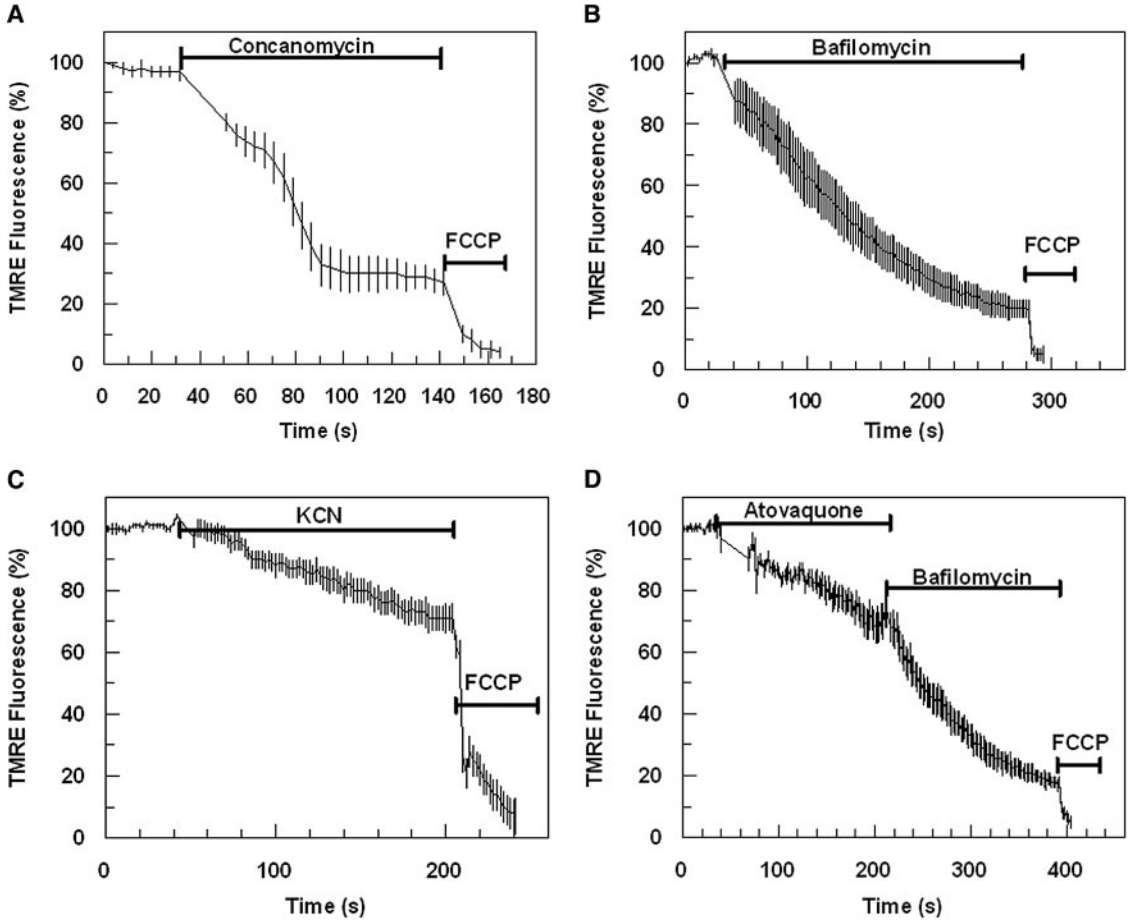

FIG. 3. Fluorescence detection of mitochondrial and plasma membrane Ψ_m components. Effect of concanomycin (200 nM) (A), bafilomycin (200 nM) (B), cyanide (10 mM) (C), and atovaquone (10 μM) (D) on TMRE-dependent parasite fluorescence. Data were normalized to 100% in untreated cells and to 0% in FCCP (10 μM)-treated cells. Graphs show means from experiments performed independently ± standard errors ($n \geq 5$).

perhaps not surprising when we consider that our recording is of an individual mitochondrion in real time.

Pharmacological validation of PfNDH2 as a drug target. The results of in vitro *P. falciparum* drug sensitivity assays using a number of ETC inhibitors including DPI and IDP are shown in Table 2.

Since both PfNDH2 and complex III are part of the *P. falciparum* mitochondrial ETC, it was of interest to determine whether the inhibition of both of these components would lead to a synergistic inhibition of the mitochondrial electron flux. To do this, we performed isobole analysis of growth inhibition by titration of the drugs at fixed ratios proportional to their IC_{50}s. In control experiments, atovaquone and proguanil yielded isobolograms indicating a synergistic interaction (Fig. 6A). Interestingly, both DPI and IDP also demonstrated a high degree of synergy with atovaquone (Fig. 6B and C). DPI antimalarial activity was also shown to be synergistic when used in combination with another complex III inhibitor, pyridone (Fig. 6E). In contrast, rotenone and atovaquone where observed to interact additively (if not slightly antagonistically) (Fig. 6D), consistent with the insensitivity of PfNDH2 to rotenone, while atovaquone in combination with either 5-FO (5-fluoroorotic acid hydrate), 3-NP (3-nitropropionic acid), or TTFA (thenoyl trifluoroacetone) resulted in additive interactions (data not shown). The interaction of DPI with proguanil (Fig. 6F) was additive.

DISCUSSION

Detection of rotenone-insensitive NADH:quinone oxidoreductase activity in *P. falciparum*. In this study, we report for the first time kinetic data for the type II NADH:quinone oxidoreductase (PfNDH2) activity from extracts of the human malaria parasite *P. falciparum*. Using the exogenous electron acceptors CoQ_1 and DB, PfNDH2 was shown to have K_m values for NADH of 16 and 5 μM, respectively (Table 1). These K_m values correspond to values reported for alternative complex I from a variety of organisms (5, 11, 17, 36) and are very similar to the values reported for the conventional complex I from various organisms and tissues (for examples, see reference 30). Our data, which indicate that *P. falciparum* NADH:quinone oxidoreductase activity is rotenone insensitive (≤50 μM), are consistent with the study by Fry and Beesley, who showed that NADH-dependent reduction of cytochrome *c* is insensitive to

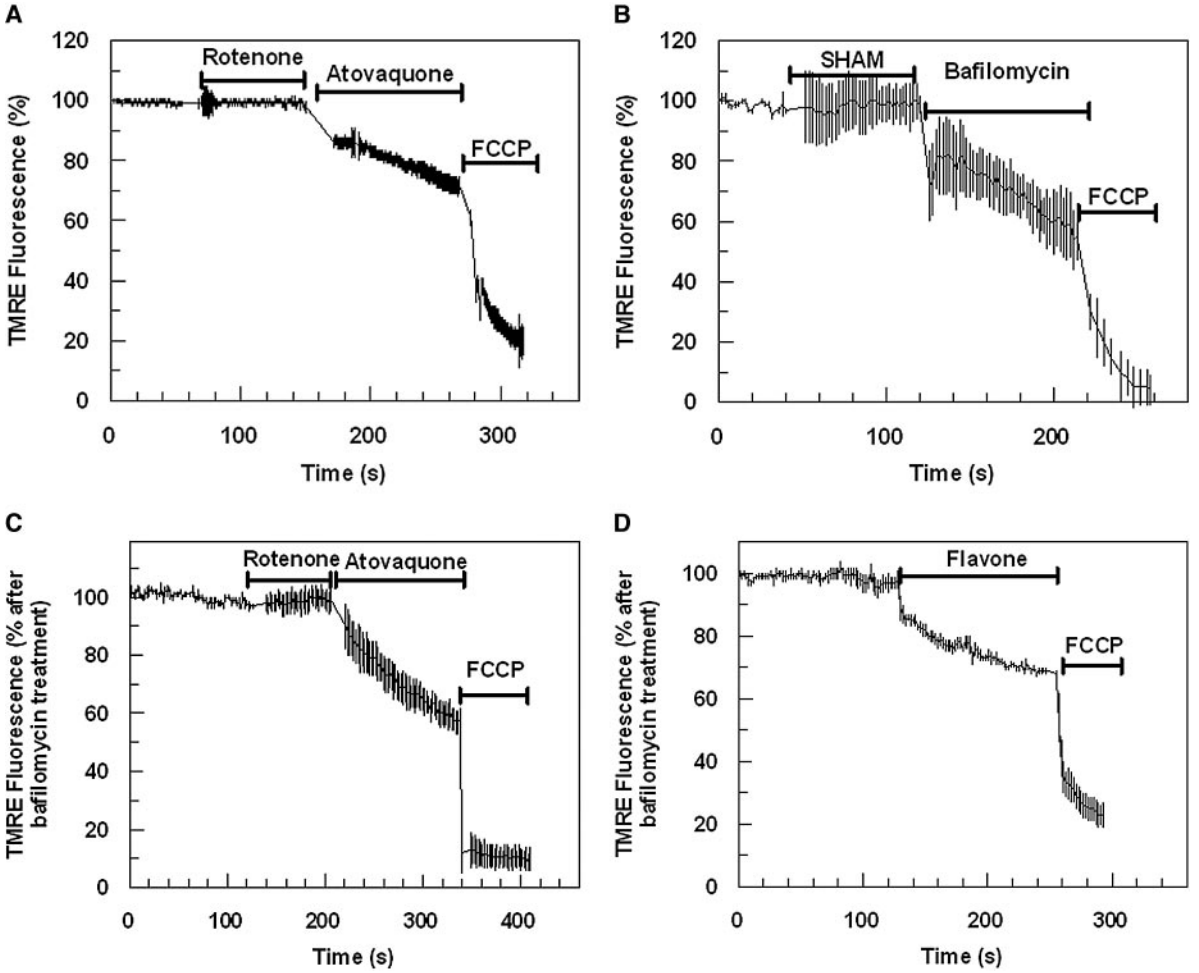

FIG. 4. Effect of mitochondrial inhibitors on mitochondrial Ψ_m. Time course of TMRE-dependent fluorescence of *P. falciparum*-infected erythrocytes after the addition of rotenone (50 μM), atovaquone (10 μM), and FCCP (10 μM) (A) and SHAM (1 mM), bafilomycin (200 nM), and FCCP (10 μM) (B). Inhibitors were also tested against bafilomycin-treated cells. Time-dependent TMRE fluorescence was monitored after addition of rotenone (50 μM), atovaquone (10 μM), and FCCP (10 μM) (C) and flavone (0.5 mM) and FCCP (10 μM) (D). Data were normalized to 100% in untreated (A and B) or bafilomycin-treated (C and D) cells and to 0% in FCCP (10 μM)-treated cells. Graphs show means from experiments performed independently ± standard errors ($n \geq 6$).

the addition of up to 80 μM rotenone (19). These biochemical studies are in turn strongly supported by data from the recently completed malaria genome project showing that the canonical NADH:dehydrogenase (complex I) is absent in *P. falciparum* (22).

In a study performed by Krungkrai et al. (28), undertaken before the completion of the malaria parasite genome (22), NADH:quinone reductase activity was reported from *P. falciparum* with a K_m for NADH similar to that reported in this study (28). In contrast to our study and that of Fry and Beesley (19), however, Krungkrai et al. reported that the NADH:quinone reductase activity was sensitive to rotenone with an IC_{50} of 12.5 μM (28). As a result of this, Krungkrai et al., concluded that the NADH:quinone reductase activity that they measured was due to the operation of NADH:dehydrogenase (complex I). Since this enzyme is absent from the parasite genome, an alternative explanation must be sought. It is possible that the discrepancy may stem from the assay conditions used for the determination of enzyme activity in the various studies. In our study, we measured enzyme kinetics in the presence of atovaquone and cyanide to stop electron flow through to the cytochrome system (complexes III and IV). Similarly, the NADH-dependent cytochrome *c* reductase activity measured by Fry and Beesley was performed in the presence of 1 mM azide (19). This procedure was not performed in the Krungkrai study, and therefore, their data may reflect a nonselective effect of rotenone. This possibility is supported by the O_2 uptake data reported by the Krungkrai study which indicate that very high concentrations of rotenone (0.33 mM) are required to attain a noncomplete (72%) reduction of mitochondrial O_2 consumption. As rotenone has been shown to inhibit NADH:dehydrogenase activity in the nanomolar range (9), it would appear that the rotenone effect described in the Krungkrai study (28) is nonselective.

PfNDH2 activity was, however, shown to be sensitive to inhibition by DPI and IDP (Fig. 1B; Table 1). DPI and IDP are general flavin reagents (9) that have been used with *Saccharomyces cerevisiae* and *Trypanosoma brucei* to inhibit rotenone-

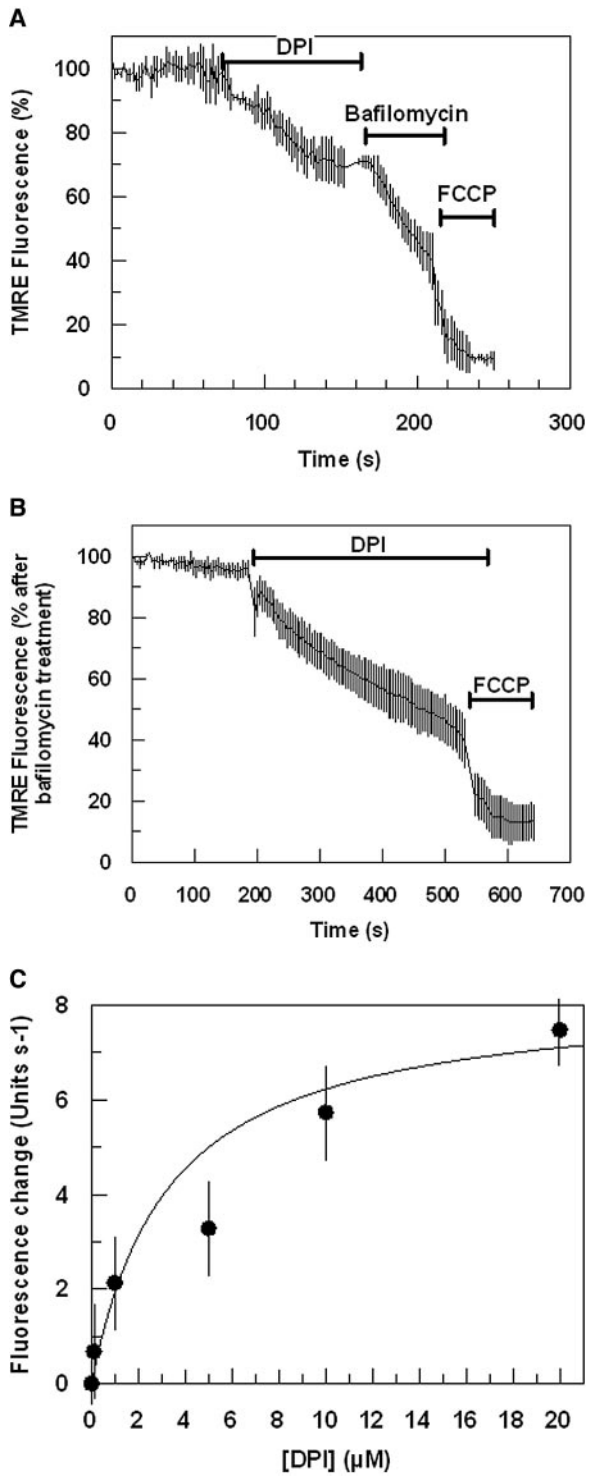

FIG. 5. Effect of DPI on *P. falciparum* mitochondrial Ψ_m. TMRE-dependent fluorescence was monitored with time after the addition of DPI (10 μM) to untreated (A) and bafilomycin-treated (B) malaria-infected erythrocytes. Data represent means from independent experiments ± standard errors ($n \geq 9$). (C) Concentration dependence of DPI on the initial rate of mitochondrial Ψ_m depolarization. Data points are means from three individual experiments. Data were fitted by nonlinear regression analysis (Marquart method) using an iterative procedure to generate the best fit (χ^2) of the curve to the data. Standard errors were calculated for each parameter using the matrix inversion method (Grafit Software).

TABLE 2. *P. falciparum* growth inhibition by mitochondrial ETC inhibitors[a]

Drug	IC_{50} (μM) (*n*)
DPI	0.24 ± 0.03 (10)
IDP	5.99 ± 0.36 (8)
Rotenone	27.02 ± 3.50 (4)
Flavone	64.24 ± 2.00 (4)
Dicumarol	113.78 ± 11.50 (4)
5-FO	0.031 ± 0.003 (5)
TTFA	20.44 ± 2.26 (7)
3-NP	158.12 ± 11.20 (6)
Atovaquone	0.001 ± 0.0002 (35)
Chloroquine	0.080 ± 0.007 (2)

[a] Values are means ± standard deviations of results from independent experiments.

insensitive NADH:quinone oxidoreductase activity (15, 17, 18). The inhibition of the flavin electron carrier by DPI and IDP is consistent with the proposed molecular structure of PfNDH2 (22). Analysis of the PfNDH2 gene (accession no. CAD51833) indicates that, as with the alternative NADH:dehydrogenases of plants, yeast, and bacteria, PfNDH2 possess two regions with a dinucleotide βαβ fold domain (25, 37). The first domain is most likely to be the region for the noncovalent attachment of the flavin adenine dinucleotide/flavin mononucleotide cofactor, while the second domain is most probably responsible for binding to NADH.

These assumptions have been supported by the homology of alternative NADH:dehydrogenases with lipoamide dehydrogenases, with which they share a high sequence similarity and probably derive from the same common ancestral flavoenzyme (25). The structure of the latter enzyme, with flavin adenine dinucleotide bound to the first dinucleotide binding βαβ fold domain, has been resolved by X-ray crystallography (34, 35). The mode of interaction with the hydrophobic ubiquinone is not clear. A tryptophan residue that is conserved in all known alternative NADH dehydrogenases has been proposed to be involved in ubiquinone binding by analogy with the bacterial photoreaction center (25). More recently, however, a study using a high-affinity inhibitor of alternative NADH dehydrogenases, 1-hydroxy-2-dodecyl-4(1H)quinolone, found that the kinetics of this enzyme follow a ping-pong mechanism (14). The study concluded that NADH and the ubiquinone headgroup (as the enzyme is not particularly discriminatory between hydrophilic and hydrophobic quinones) interact at the same binding pocket in an alternating fashion (14).

A number of alternative NADH dehydrogenases contain insertions with homology to Ca^{2+}-binding EF-hand motifs (25, 36, 40). Clustal analysis of PfNDH2 with EF-hand containing alternative NADH dehydrogenases does not indicate the presence of conserved EF-hand domains. However, it should be noted that these insertions are not always found at similar positions within the enzymes and it remains to be determined whether PfNDH2 is Ca^{2+} dependent.

PfNDH2 is an essential component for the generation of mitochondrial Ψ_m. In this study, we have developed a robust assay for the real-time, single-cell measurement of plasma membrane and mitochondrial Ψ_m in *P. falciparum*-parasitized erythrocytes. The accumulation into parasites of the Ψ_m-sensitive probe TMRE was demonstrated to be driven by two

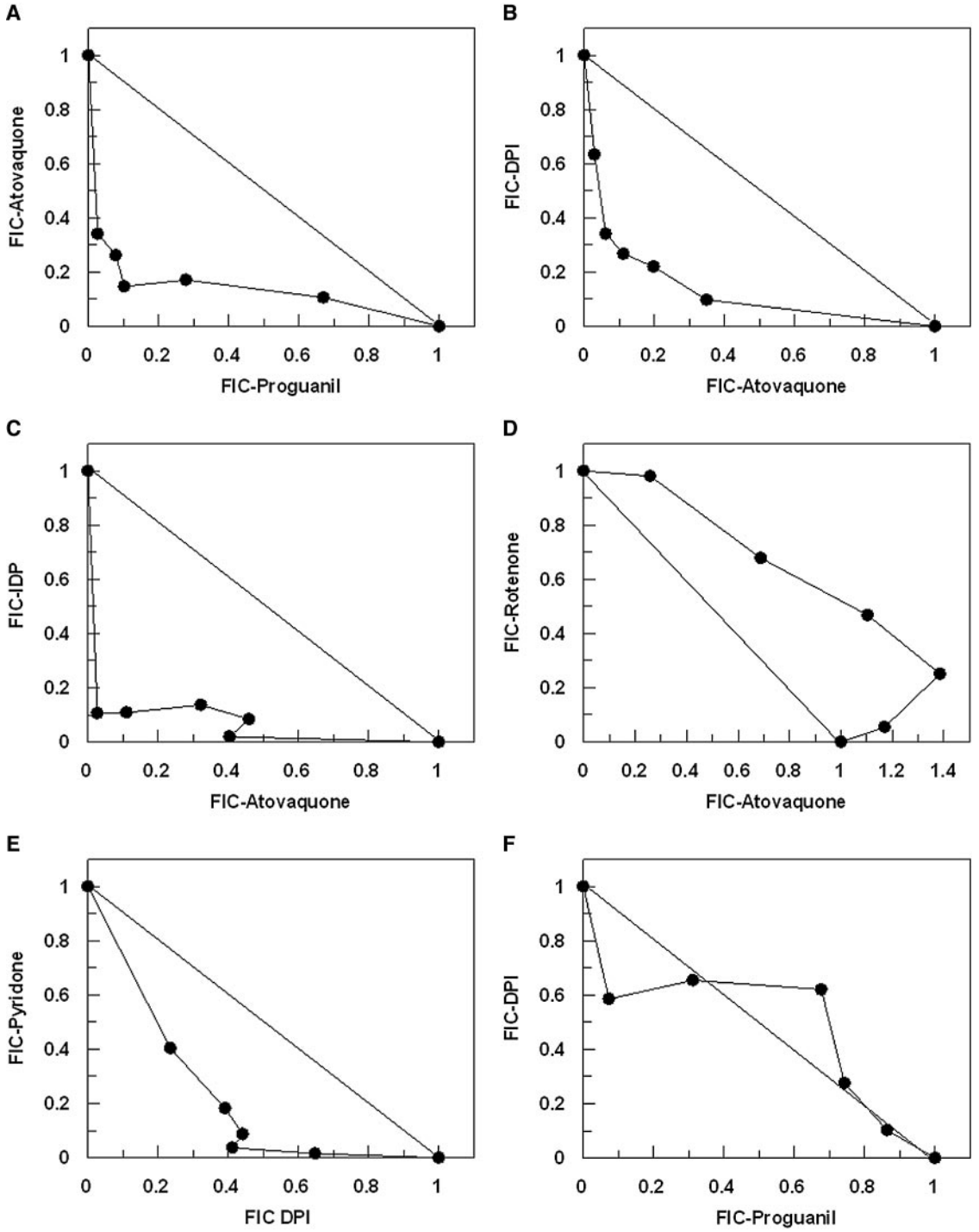

FIG. 6. Isobole analysis of mitochondrial inhibitors on antimalarial activity. The fractional inhibitory concentrations of IC_{50} values for drugs in combination are shown for atovaquone versus proguanil (A), atovaquone versus DPI (B), atovaquone versus IDP (C), atovaquone versus rotenone (D), DPI versus pyridone (E), and DPI versus proguanil (F). Data are means of results from four independent experiments.

major components. The first of these, representing some 70 to 80% of the total cellular fluorescence signal, was shown to be bafilomycin and concanomycin sensitive (Fig. 2a to e and 3a and b), both known inhibitors of V-type H^+ ATPases. This therefore represents the contribution of the V-type H^+ ATPase operating on the plasma membrane of the parasite which actively extrudes protons for the regulation of intracellular pH (41), generating a high (approximately −100 mV) transmembrane Ψ_m (1). The second driving force for TMRE accumulation was shown to be bafilomycin insensitive but sensitive to ETC inhibitors such as azide and cyanide (Fig. 2a to e and 3C and D). These data clearly demonstrate that this com-

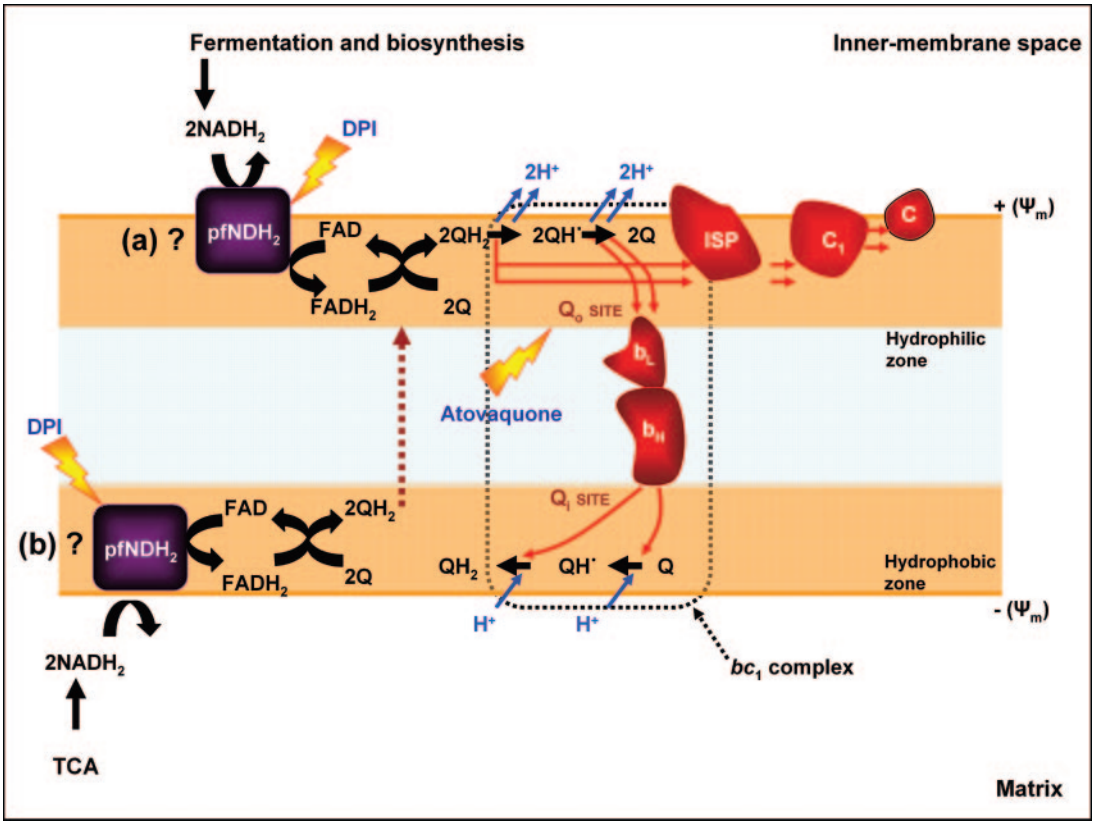

FIG. 7. Schematic representation of PfNDH2 function in the *P. falciparum* mitochondrial ETC. The exact location of PfNDH2 is not known; in the schematic it is shown as localized on either the cytosolic (a) or the matrix (b) side of the mitochondrial inner membrane. Inhibition of PfNDH2 and the bc_1 complex (lighting bolts) has been shown to be synergistic, probably by affecting the redox reactions of the Q cycle.

ponent represents the contribution from the single mitochondrion found inside the malaria parasite.

In line with previous studies (46), the bc_1 complex inhibitor atovaquone was shown to collapse the Ψ_m of *P. falciparum* mitochondria (Fig. 3C and 4A). However, as shown for the rodent malaria parasite *P. yoelii* (49), the addition of rotenone (50 μM) had no depolarizing effect (Fig. 4A and C). The presence of a rotenone-insensitive generation of mitochondrial Ψ_m in *P. falciparum* is consistent with our enzyme kinetic data of PfNDH2, which also showed a lack of effect from rotenone. Interestingly, a collapse of mitochondrial Ψ_m was observed upon addition of DPI or flavone (Fig. 4D and 5A to C) as well as IDP (not shown). These inhibitors have been demonstrated in previous studies with *P. yoelii*, *T. brucei*, and *S. cerevisiae* to inhibit alternative NADH:dehydrogenases (11, 15, 17, 18, 49).

The absence of transmembrane domains in alternative NADH:dehydrogenases corroborates the observation that, unlike conventional NADH:dehydrogenases, these enzymes are not involved directly in proton pumping (25, 36, 40). However, as several organisms (e.g., *S. cerevisiae*) only contain alternative NADH:dehydrogenases in their mitochondrial ETC, it has been suggested that their activity may indirectly contribute to the formation of an electrochemical Ψ_m (36). The data presented in this study, revealing a collapse of mitochondrial Ψ_m by the DPI- or IDP-mediated inhibition of PfNDH2 (Fig. 5A to C), strongly support the hypothesis for a role of PfNDH2 in mitochondrial Ψ_m formation.

Presently, we do not know whether PfNDH2 operates on the internal or external face of the mitochondrial inner membrane. We now know that inhibition of this enzyme leads to a depolarization of the Ψ_m and we can hypothesize that this is as a result of a decrease in the levels of ubiquinol (QH2), which subsequently enters the Q-cycle in the bc_1 complex (Fig. 7) (7, 8, 24). However, there is also the possibility that PfNDH2 can generate a transmembrane Ψ_m via a redox-linked "loop," since both ubiquinone (Q) and QH2 are able to traverse the lipid bilayer (Fig. 7).

The functioning of PfNDH2 relies on a ready source of reduction equivalents [NAD(P)H2], and since the intraerythrocytic parasites are believed to have a rather inactive tricarboxylic acid cycle (19, 21, 50), we predict that PfNDH2 is localized on the external face, oxidizing NAD(P)H from the cytosol. A major source of parasite cytosolic NADH is glycolysis, but the operation of lactate dehydrogenase essentially renders this process redox neutral (21). However, there are additional substantial sources of NADH from general biosynthetic processes during cell growth (39) which may be providing reducing power for PfNDH2.

Inhibition of PfNDH2 is lethal to *P. falciparum*. IDP was shown to inhibit PfNDH2 activity with an IC_{50} of 66 μM and collapse mitochondrial membrane potential at ~1 μM. The IC_{50} for growth inhibition, however, was measured at ~3 μM. In the case of DPI, the IC_{50} for growth inhibition was measured at 240 nM, while the mitochondrial Ψ_m was shown to be

sensitive to ≥1 μM DPI. These values are in comparison to an IC_{50} for PfNDH2 inhibition of 15 μM (with DB as an electron acceptor) (Table 2). There is a discrepancy here, as, in most circumstances, the drug concentration required to inhibit enzyme activity is the same or lower than that required to inhibit growth proliferation. However, in the case of type II NADH:dehydrogenases, the enzyme activity is measured with artificial electron acceptors, and this greatly influences the effect of inhibitors (17). In *Trypanosoma brucei*, for example, the inhibitory effect of IDP against the type II NADH:dehydrogenase varied from total inhibition using CoQ_2 with 50 μM IDP to incomplete inhibition (maximum of 66% inhibition) with the acceptor DCPIP (dichlorophenol-indophenol) (17). Similar low inhibitory effects of IDP were observed with ferricyanide as the electron acceptor (17). Comparing enzyme activity with antimalarial activity is not always particularly informative when very different conditions have been employed to measure the two parameters. This is probably true here, where the enzyme inhibitory activities of compounds are measured using initial rates over 10 min using an artificial electron acceptor and antimalarial activity is measured using intact organisms over 48 h of exposure. It cannot be ruled out, of course, that DPI has additional nonselective inhibitory effects on *P. falciparum* growth, and these may go some way in explaining this discrepancy. However, until we perform gene knockout studies or more detailed biochemical studies with purified and/or recombinant PfNDH2, this argument remains speculative.

Support for PfNDH2 being the target for DPI and IDP antimalarial activity was provided by drug sensitivity experiments performed with the complex III inhibitors atovaquone and pyridone. The fractional inhibitory concentrations of resulting IC_{50}s plotted as isobolograms clearly reveal a high degree of synergy when DPI (or IDP) is used in combination with either atovaquone or pyridone (Fig. 6B, C, and E). These data can most simply be interpreted as a result of the two drugs inhibiting the same function (electron flux) but at different points, in this case the Q-cycle between alternative complex I and complex III (Fig. 7).

As DPI and IDP are general flavin reagents, it is anticipated that they would be of no clinical use due to selectivity issues. However, DPI and IDP have been very valuable tools in providing proof-of-concept pharmacological data on the suitability of PfNDH2 as a chemotherapeutic target. Targeting this enzyme promises to be an attractive strategy, particularly given that alternative NADH:dehydrogenases are absent from human mitochondria (36). Structure and activity studies using both medicinal chemistry and in silico modeling approaches have recently begun in our laboratories. It is our hope that the translation of these studies will yield promising drug candidates in the near future. It is worth noting that, in a very recent study, a therapeutic strategy similar to that described here has been adopted toward the treatment of tuberculosis (52).

ACKNOWLEDGMENTS

G.A.B. is supported by an Early Career Leverhulme Trust Fellowship. P.V. acknowledges support from the Royal Thai Government. P.G.B., P.M.O., and S.A.W. are supported by BBSRC, MRC, and Wellcome Trust grants.

We thank the staff and patients of Ward 7Y and the Gastroenterology Unit, Royal Liverpool Hospital, for their generous donation of blood.

REFERENCES

1. **Allen, R. J., and K. Kirk.** 2004. The membrane potential of the intraerythrocytic malaria parasite plasmodium falciparum. J. Biol. Chem. **279:**11264–11272.
2. **Berenbaum, M. C.** 1978. A method for testing for synergy with any number of agents. J. Infect. Dis. **137:**122–130.
3. **Biagini, G. A., D. Lloyd, K. Kirk, and M. R. Edwards.** 2000. The membrane potential of Giardia intestinalis. FEMS Microbiol. Lett. **192:**153–157.
4. **Biagini, G. A., P. M. O'Neill, A. Nzila, S. A. Ward, and P. G. Bray.** 2003. Antimalarial chemotherapy: young guns or back to the future? Trends Parasitol. **19:**479–487.
5. **Bjorklof, K., V. Zickermann, and M. Finel.** 2000. Purification of the 45 kDa, membrane bound NADH dehydrogenase of Escherichia coli (NDH-2) and analysis of its interaction with ubiquinone analogues. FEBS Lett. **467:**105–110.
6. **Breman, J. G.** 2001. The ears of the hippopotamus: manifestations, determinants, and estimates of the malaria burden. Am. J. Trop. Med. Hyg. **64:**1–11.
7. **Crofts, A. R.** 2004. The cytochrome bc1 complex: function in the context of structure. Annu. Rev. Physiol. **66:**689–733.
8. **Crofts, A. R.** 2004. Proton-coupled electron transfer at the Qo-site of the bc1 complex controls the rate of ubihydroquinone oxidation. Biochim. Biophys. Acta **1655:**77–92.
9. **Degli Esposti, M.** 1998. Inhibitors of NADH-ubiquinone reductase: an overview. Biochim. Biophys. Acta **1364:**222–235.
10. **Desjardins, R. E., C. J. Canfield, J. D. Haynes, and J. D. Chulay.** 1979. Quantitative assessment of antimalarial activity in vitro by a semiautomated microdilution technique. Antimicrob. Agents Chemother. **16:**710–718.
11. **de Vries, S., and L. A. Grivell.** 1988. Purification and characterization of a rotenone-insensitive NADH:Q6 oxidoreductase from mitochondria of Saccharomyces cerevisiae. Eur. J. Biochem. **176:**377–384.
12. **Divo, A. A., T. G. Geary, J. B. Jensen, and H. Ginsburg.** 1985. The mitochondrion of Plasmodium falciparum visualized by rhodamine 123 fluorescence. J. Protozool. **32:**442–446.
13. **Ellis, J. E.** 1994. Coenzyme Q homologs in parasitic protozoa as targets for chemotherapeutic attack. Parasitol. Today **10:**296–301.
14. **Eschemann, A., A. Galkin, W. Oettmeier, U. Brandt, and S. Kerscher.** 2005. HDQ (1-hydroxy-2-dodecyl-4(1H)quinolone), a high affinity inhibitor for mitochondrial alternative NADH dehydrogenase: evidence for a ping-pong mechanism. J. Biol. Chem. **280:**3138–3142.
15. **Fang, J., and D. S. Beattie.** 2003. External alternative NADH dehydrogenase of Saccharomyces cerevisiae: a potential source of superoxide. Free Radic. Biol. Med. **34:**478–488.
16. **Fang, J., and D. S. Beattie.** 2003. Identification of a gene encoding a 54 kDa alternative NADH dehydrogenase in Trypanosoma brucei. Mol. Biochem. Parasitol. **127:**73–77.
17. **Fang, J., and D. S. Beattie.** 2002. Novel FMN-containing rotenone-insensitive NADH dehydrogenase from Trypanosoma brucei mitochondria: isolation and characterization. Biochemistry **41:**3065–3072.
18. **Fang, J., and D. S. Beattie.** 2002. Rotenone-insensitive NADH dehydrogenase is a potential source of superoxide in procyclic Trypanosoma brucei mitochondria. Mol. Biochem. Parasitol. **123:**135–142.
19. **Fry, M., and J. E. Beesley.** 1991. Mitochondria of mammalian Plasmodium spp. Parasitology **102**(Pt. 1)**:**17–26.
20. **Fry, M., and M. Pudney.** 1992. Site of action of the antimalarial hydroxynaphthoquinone, 2-[trans-4-(4′-chlorophenyl) cyclohexyl]-3-hydroxy-1,4-naphthoquinone (566C80). Biochem. Pharmacol. **43:**1545–1553.
21. **Fry, M., E. Webb, and M. Pudney.** 1990. Effect of mitochondrial inhibitors on adenosinetriphosphate levels in Plasmodium falciparum. Comp. Biochem. Physiol. B **96:**775–782.
22. **Gardner, M. J., N. Hall, E. Fung, O. White, M. Berriman, R. W. Hyman, J. M. Carlton, A. Pain, K. E. Nelson, S. Bowman, I. T. Paulsen, K. James, J. A. Eisen, K. Rutherford, S. L. Salzberg, A. Craig, S. Kyes, M. S. Chan, V. Nene, S. J. Shallom, B. Suh, J. Peterson, S. Angiuoli, M. Pertea, J. Allen, J. Selengut, D. Haft, M. W. Mather, A. B. Vaidya, D. M. Martin, A. H. Fairlamb, M. J. Fraunholz, D. S. Roos, S. A. Ralph, G. I. McFadden, L. M. Cummings, G. M. Subramanian, C. Mungall, J. C. Venter, D. J. Carucci, S. L. Hoffman, C. Newbold, R. W. Davis, C. M. Fraser, and B. Barrell.** 2002. Genome sequence of the human malaria parasite Plasmodium falciparum. Nature **419:**498–511.
23. **Gazarini, M. L., and C. R. Garcia.** 2004. The malaria parasite mitochondrion senses cytosolic Ca2+ fluctuations. Biochem. Biophys. Res. Commun. **321:**138–144.
24. **Hunte, C., H. Palsdottir, and B. L. Trumpower.** 2003. Protonmotive pathways and mechanisms in the cytochrome bc1 complex. FEBS Lett. **545:**39–46.
25. **Kerscher, S. J.** 2000. Diversity and origin of alternative NADH:ubiquinone oxidoreductases. Biochim. Biophys. Acta **1459:**274–283.
26. **Krungkrai, J.** 2004. The multiple roles of the mitochondrion of the malarial parasite. Parasitology **129:**511–524.
27. **Krungkrai, J.** 1995. Purification, characterization and localization of mito-

chondrial dihydroorotate dehydrogenase in Plasmodium falciparum, human malaria parasite. Biochim. Biophys. Acta **1243:**351–360.
28. **Krungkrai, J., R. Kanchanarithisak, S. R. Krungkrai, and S. Rochanakij.** 2002. Mitochondrial NADH dehydrogenase from Plasmodium falciparum and Plasmodium berghei. Exp. Parasitol. **100:**54–61.
29. **Lambros, C., and J. P. Vanderberg.** 1979. Synchronization of Plasmodium falciparum erythrocytic stages in culture. J. Parasitol. **65:**418–420.
30. **Lenaz, G., R. Fato, A. Baracca, and M. L. Genova.** 2004. Mitochondrial quinone reductases: complex I. Methods Enzymol. **382:**3–20.
31. **Looareesuwan, S., P. Wilairatana, K. Chalermarut, Y. Rattanapong, C. J. Canfield, and D. B. Hutchinson.** 1999. Efficacy and safety of atovaquone/proguanil compared with mefloquine for treatment of acute Plasmodium falciparum malaria in Thailand. Am. J. Trop. Med. Hyg. **60:**526–532.
32. **Luttik, M. A., K. M. Overkamp, P. Kotter, S. de Vries, J. P. van Dijken, and J. T. Pronk.** 1998. The Saccharomyces cerevisiae NDE1 and NDE2 genes encode separate mitochondrial NADH dehydrogenases catalyzing the oxidation of cytosolic NADH. J. Biol. Chem. **273:**24529–24534.
33. **Marres, C. A., S. de Vries, and L. A. Grivell.** 1991. Isolation and inactivation of the nuclear gene encoding the rotenone-insensitive internal NADH:ubiquinone oxidoreductase of mitochondria from Saccharomyces cerevisiae. Eur. J. Biochem. **195:**857–862.
34. **Mattevi, A., G. Obmolova, J. R. Sokatch, C. Betzel, and W. G. Hol.** 1992. The refined crystal structure of Pseudomonas putida lipoamide dehydrogenase complexed with NAD+ at 2.45 A resolution. Proteins **13:**336–351.
35. **Mattevi, A., A. J. Schierbeek, and W. G. Hol.** 1991. Refined crystal structure of lipoamide dehydrogenase from Azotobacter vinelandii at 2.2 A resolution. A comparison with the structure of glutathione reductase. J. Mol. Biol. **220:**975–994.
36. **Melo, A. M., T. M. Bandeiras, and M. Teixeira.** 2004. New insights into type II NAD(P)H:quinone oxidoreductases. Microbiol. Mol. Biol. Rev. **68:**603–616.
37. **Michalecka, A. M., S. C. Agius, I. M. Moller, and A. G. Rasmusson.** 2004. Identification of a mitochondrial external NADPH dehydrogenase by overexpression in transgenic Nicotiana sylvestris. Plant J. **37:**415–425.
38. **Murphy, A. D., J. E. Doeller, B. Hearn, and N. Lang-Unnasch.** 1997. Plasmodium falciparum: cyanide-resistant oxygen consumption. Exp. Parasitol. **87:**112–120.
39. **Overkamp, K. M., B. M. Bakker, P. Kotter, A. van Tuijl, S. de Vries, J. P. van Dijken, and J. T. Pronk.** 2000. In vivo analysis of the mechanisms for oxidation of cytosolic NADH by *Saccharomyces cerevisiae* mitochondria. J. Bacteriol. **182:**2823–2830.
40. **Rasmusson, A. G., K. L. Soole, and T. E. Elthon.** 2004. Alternative NAD(P)H dehydrogenases of plant mitochondria. Annu. Rev. Plant Biol. **55:**23–39.
41. **Saliba, K. J., and K. Kirk.** 1999. pH regulation in the intracellular malaria parasite, Plasmodium falciparum. H(+) extrusion via a v-type h(+)-atpase. J. Biol. Chem. **274:**33213–33219.
42. **Schnell, J. V., W. A. Siddiqui, and Q. M. Geiman.** 1971. Biosynthesis of coenzymes Q by malarial parasites. 2. Coenzyme Q synthesis in blood cultures of monkeys infected with malarial parasites (Plasmodium falciparum and P. knowlesi). J. Med. Chem. **14:**1026–1029.
43. **Skelton, F. S., K. D. Lunan, K. Folkers, J. V. Schnell, W. A. Siddiqui, and Q. M. Geiman.** 1969. Biosynthesis of ubiquinones by malarial parasites. I. Isolation of [14C]ubiquinones from cultures of rhesus monkey blood infected with Plasmodium knowlesi. Biochemistry **8:**1284–1287.
44. **Snow, R. W., C. A. Guerra, A. M. Noor, H. Y. Myint, and S. I. Hay.** 2005. The global distribution of clinical episodes of Plasmodium falciparum malaria. Nature **434:**214–217.
45. **Snow, R. W., J. F. Trape, and K. Marsh.** 2001. The past, present and future of childhood malaria mortality in Africa. Trends Parasitol. **17:**593–597.
46. **Srivastava, I. K., H. Rottenberg, and A. B. Vaidya.** 1997. Atovaquone, a broad spectrum antiparasitic drug, collapses mitochondrial membrane potential in a malarial parasite. J. Biol. Chem. **272:**3961–3966.
47. **Trager, W., and J. B. Jensen.** 1976. Human malaria parasites in continuous culture. Science **193:**673–675.
48. **Uyemura, S. A., S. Luo, S. N. Moreno, and R. Docampo.** 2000. Oxidative phosphorylation, Ca(2+) transport, and fatty acid-induced uncoupling in malaria parasites mitochondria. J. Biol. Chem. **275:**9709–9715.
49. **Uyemura, S. A., S. Luo, M. Vieira, S. N. Moreno, and R. Docampo.** 2004. Oxidative phosphorylation and rotenone-insensitive malate- and NADH-quinone oxidoreductases in Plasmodium yoelii yoelii mitochondria in situ. J. Biol. Chem. **279:**385–393.
50. **Vaidya, A. B.** 2004. Mitochondrial and plastid functions as antimalarial drug targets. Curr. Drug Targets Infect. Disord. **4:**11–23.
51. **van Dooren, G. G., M. Marti, C. J. Tonkin, L. M. Stimmler, A. F. Cowman, and G. I. McFadden.** 2005. Development of the endoplasmic reticulum, mitochondrion and apicoplast during the asexual life cycle of Plasmodium falciparum. Mol. Microbiol. **57:**405–419.
52. **Weinstein, E. A., T. Yano, L. S. Li, D. Avarbock, A. Avarbock, D. Helm, A. A. McColm, K. Duncan, J. T. Lonsdale, and H. Rubin.** 2005. Inhibitors of type II NADH:menaquinone oxidoreductase represent a class of antitubercular drugs. Proc. Natl. Acad. Sci. USA **102:**4548–4553.
53. **Yagi, T.** 1991. Bacterial NADH-quinone oxidoreductases. J. Bioenerg. Biomembr. **23:**211–225.
54. **Yeh, I., T. Hanekamp, S. Tsoka, P. D. Karp, and R. B. Altman.** 2004. Computational analysis of Plasmodium falciparum metabolism: organizing genomic information to facilitate drug discovery. Genome Res. **14:**917–924.